NUCL SCI TECH (2018) 29:180
https://doi.org/10.1007/s41365-018-0514-x

Fast-bunching design of compact heavy ion RFQ linac

Ke-Dong Wang[1,2,3] · You-Jin Yuan[1] · Xue-Jun Yin[1,3] · Jian-Cheng Yang[1] · Heng Du[1,3] · Zhong-Shan Li[1,3] · Xiao-Ni Li[1,3] · He Zhao[1,2,3] · Zi-Qiang Dong[1,2,3] · Jie Liu[1,2,3] · Jia-Wen Xia[1,3]

Received: 11 April 2018 / Revised: 28 May 2018 / Accepted: 23 June 2018 / Published online: 23 November 2018

Abstract We propose the construction of a compact linac as the injector of a cancer therapy facility at the Institute of Modern Physics (IMP) of the Chinese Academy of Sciences (CAS). Based on a traditional setup, a new compact fast-bunching design is first introduced to optimize the 600 keV/u RFQ with a 0.05 pmA $^{12}C^{4+}$ beam. This shortens the RFQ structure length from the standard design value of 272–230 cm while effectively regulating the particle loss and emittance growth. In addition, a detailed error analysis was performed after the optimization process. The error sources cover input beam parameters errors, machining errors and alignment errors. The simulation results show that the beam loss and emittance growth of the RFQ are acceptable and within typical ranges of error.

Keywords Linac · RFQ · Beam dynamics design · Fast-bunching

This work was supported by the National Natural Science Foundation of China (No. 11375243) and the Guangdong Innovative and Entrepreneurial Research Team Program (No. 2016ZT06G373).

✉ Xue-Jun Yin
yinxj@impcas.ac.cn

1 Institute of Modern Physics, Chinese Academy of Sciences, Lanzhou 730000, China

2 University of Chinese Academy of Sciences, Beijing 100049, China

3 Huizhou Research Center of Ion Science, Huizhou 516003, China

1 Introduction

The RFQ is an essential component of the linac and has a significant advantage with respect to the acceleration of beams with low velocity in the typical range of approximately 0.01–0.06 times the speed of light [1]. In recent years, many compact accelerators have utilized RFQ as injectors in many fields such as cancer therapy research and other radiation-based applications. For instance, hadron radiotherapy has gradually been developed in clinics, and many facilities have been built around the world such as in Germany [2], Japan [3, 4] and China [5, 6]. The injection and extraction energy parameters of some of these RFQ injectors are listed in Table 1 [7].

Recently, a new linac injector for the carbon ion therapy facility was proposed and designed by IMP. It consists of an ECR ion source, a 162.5 MHz RFQ, a compact Interdigital H-mode Drift-Tube-Linac (IH-DTL), and beam transport lines. The layout of the linac is shown in Fig. 1. The RFQ operates at 0.1% duty factor and accelerates a $^{12}C^{4+}$ beam from 8 to 600 keV/u with a peak current of 0.05 pmA (0.2 emA). In the design process, the peak current is set to 0.1 pmA to maintain current tolerance.

The dynamics design of the RFQ, which is mainly directed against space-charge effects, has been extensively investigated worldwide over many years [8–12]. However, the requirement of a compact structure is considered to be more important in most radiotherapy facilities than the suppression of the space-charge effect. In such facilities, the structure size impacts cost and can pose construction challenges. In this report, the optimization of the RFQ design will be investigated based on the Gentle-bunching (GB) section of the Four-section design. A new fast-bunching section is introduced to replace the GB

Table 1 Parameters of RFQ of heavy ion radio therapy facilities

Institute/hospital	Name of facility	Location Country	Injection energy (keV/u)	Extraction energy (keV/u)
Heidelberg	HICAT	Germany	8	400
CCLRC	PARMELA	Warrington	8	382
CNAO	CNAO	Italy	8	400
NIRS	HIMAC	Japan	8	600
Gunma Univ.	GHMC	Japan	10	400

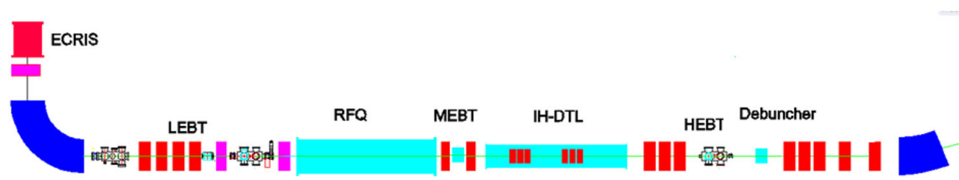

Fig. 1 Layout of the cancer therapy facility (Color online)

section. This results in a compact design of the RFQ while keeping particle loss and emittance growth well controlled.

2 Dynamics design

The dynamics design of the RFQ can be performed using the code PARMTEQM [13] which is widely used [14, 15], and important parameters such as the input energy and the inter-vane voltage should be defined in advance.

In the design process, a high input energy results in a long RFQ cavity due to the cell length and the effect of the bunching process, which generally leads to a decrease in the accelerating gradient of the RFQ. The ion source extraction voltage is usually chosen to be 20–30 kV for the C^{4+} ions as shown in Table 2 [7]. The extraction voltage of this source should be chosen to match two conditions: One is an adequate beam intensity with a relatively good quality and the other is a reduction of the sparking risk. A suitable inter-vane voltage is required in an RFQ to effectively maintain the radial focusing strength and accelerating gradient. However, this value is restricted by the maximum surface field of the electrode. Finally, the inter-vane voltage is chosen in the range of 70–80 kV.

Table 2 Carbon ion sources for RFQs in the facilities under operation or being commissioned

Name of facility	Charge state of C ions	Extraction voltage (kV)
HIMAC	2 +/4 +	48/24
HIBMC	4 +	25
HIRFL-CSR	4 +	20
HIT	4 +	24
GHMC	4 +	30
CNAO	4 +	24
PTC-Marburg	4 +	24
NRoCK	4 +	24

A basic dynamics design of the proposed RFQ was performed by PARMTEQM after reiterating the important parameters previously mentioned. However, a few problems were encountered. For example, the beam size could not be well controlled when it entered the GB section as shown as in Fig. 7, which impacts the transmission efficiency and the beam quality due to abrupt changes in certain parameters and phase advance resonances. On the other hand, the length of the electrode is 2.7 m. The fabrication of such an electrode in one segment will be difficult in standard machining environments. Thus, the best approach is to reduce the length or separate the electrodes into segments for machining.

The optimization procedure was repeated to achieve an optimal design with a maximum transmission efficiency, and a minimum emittance growth and structure length. Some specifications and constraints are listed as follows:

1. For the proposed RFQ operating with 0.1% duty factor, the maximum surface field is constrained to lower than 27.2 MV/m. This corresponds to a Kilpatrick factor [16] of less than 2.0 at 162.5 MHz.
2. The structure length should be less than 2.5 m to minimize construction costs and power requirement.
3. Beam transmission efficiency should be as high as possible.
4. Phase advance resonances should be avoided.

Parametric resonance and coupling between the transverse and the longitudinal phase space are avoided by changing the focusing factor B along the cells. The B changes with the transverse RF defocusing force to maintain the transverse beam movement in dynamic balance [10, 17]. In addition, abrupt changes in parameters at the junctions are smoothed to improve the transmission efficiency [8].

The traditional RFQ dynamics design is based on Kapchinsky's adiabatic bunching condition [18]. Under this condition, the geometric length of the separatrix is almost constant in spite of the increase in the velocity of particles, which can reduce the impact of the space-charge effect. In a traditional design, the RFQ is divided into four sections: radial matching, shaping, gentle bunching (GB), and accelerating sections. The GB section where the Kapchinsky's condition is applied could be further divided into pre-bunching (small m and slow m ramping) and bunching (fast m ramping) sections [19].

The space-charge effect is not strong in the proposed RFQ for a compact linac design, and the GB section can be shortened to preserve length for the accelerating section. A short fast-bunching section is introduced to substitute for the long adiabatic pre-bunching section. The parameter S which is almost proportional to the separatrix area is used for the optimization of the fast-bunching section. S is defined as [19]:

$$S = \sqrt{|\Delta|}\beta^2\gamma^3 g(\phi s), \tag{1}$$

where,

$$\Delta = \frac{\pi^2 qAV\sin(\phi s)}{2mc^2\beta^2}, \tag{2}$$

$$g(\phi s) = (\psi/2\pi)\sqrt{1-\phi s\cot(\phi s)}, \tag{3}$$

A is the accelerating efficiency, V is the inter-vane voltage, ϕs is the synchronous phase angle, ψ is the phase width, β is the synchronous velocity, γ is the Lorentz factor, q is the charge, and m is the rest mass of the ion.

An increase in S is important in forming a good beam bunch under the influence of a strong space-charge force. However, for low-current dynamics, this parameter could be kept at a constant, which facilitates faster beam bunching with sufficiently high transmission [19].

The parameter S can be kept almost constant in the fast-bunching section through optimization of the modulation factor m and the synchronous phase angle ϕs. The modulation factor grows faster compared to the case of a traditional design. Figure 2 shows the optimized parameter curves of the fast-bunching section. When the optimized m factor of the fast-bunching is compared with a traditional m factor, the platform at the pre-bunching section almost vanishes. Moreover, the entire length of the RFQ is shortened based on the premise of ensuring particle transport, and the RFQ acceleration efficiency is increased.

Additionally, the shaping section is optimized to allow the beam to transmit effectively during the fast-bunching process. In this section, the m factor is optimized to a relatively low value, which decreases the separatrix height in the RFQ entrance and maintains a sufficient acceptance for the input beam.

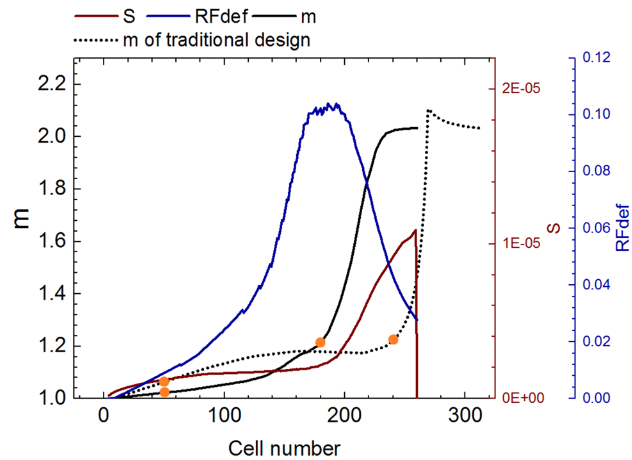

Fig. 2 The parameter curves of the optimized fast-bunching section. The m curve of the pre-bunching section is shown using dots for comparison. The start and end points of the fast-bunching and pre-bunching sections are indicated by the solid orange circles (Color online)

Fast-bunching is used to create a more compact structure by ignoring the space-charge effect. As the beam current is increased, the fast-bunching process terminates, and therefore, the current limits the application range of the fast-bunching design. Figure 3 shows the impact of an increase inthe current in the fast-bunching process. The beam experiences dispersion in the longitudinal phase space, since the longitudinal phase advance decreases as the space-charge effect increases. This impacts the beam transmission and quality in the bunching process. The current should be lower than 1.0 pmA in the design of the 162.5 MHz RFQ. This can be realized by analyzing the influence of the current increase on the fast-bunching process.

Figure 4 and Table 3 show the parameters of the 162.5 MHz RFQ dynamics design after optimization. The final Kilpatrick factor of the design is 1.83. In the case of the fast-bunching design, phase advance resonances are avoided, the transmission efficiency is increased, and the structure length is shortened. A transmission efficiency of 99.3% is obtained with an RFQ length of 230 cm.

The simulation results of the PARMTEQM are shown in Figs. 5 and 6. The number of particles in the simulation is 10,000. The particles are judged to be lost when their energy deviates from that of the synchrotron particle by more than 5%. The sum of the lost particles and transverse emittance is clearly reduced in the optimized design as shown in Fig. 7. It is observed that the loss peak in the optimization design occurs at approximately cell-180, because the fast-bunching process causes the separatrix to shrink quickly. The particles at the edge of the separatrix

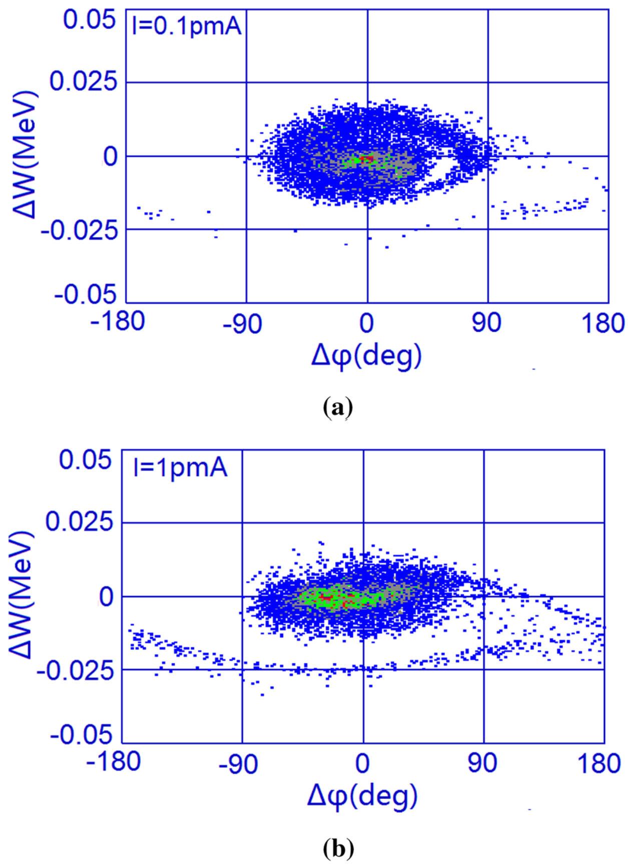

Fig. 3 The longitudinal phase space at the 140th cell (near the end of the bunching section) for different beam currents (Color online)

will be lost longitudinally when the beam enters the accelerating section.

3 Error analysis

The tolerance of the RFQ for a non-ideal input beam directly influenced the beam stability and quality. Both the operating stability of the ion source and the ripple of the LEBT power supplies impact the beam parameters at the RFQ entrance [20–22]. It is difficult to adjust the parameters of the beam to satisfy dynamics design during actual operation. Consequently, it is necessary to perform the error analysis at the entrance of the RFQ. The results are shown in Fig. 8.

The design values of the beam parameters at the entrance of the RFQ are $\varepsilon_t = 0.2\,\pi\text{mm}\cdot\text{mrad}$ (Norm. RMS), the beam current of 0.1 pmA, and the energy of 8 keV/u with zero energy spread and 360° phase width. The controlling variables method was used during the simulation. One of the parameters such as the emittance, current or energy spread of the input beams is adjusted while the other parameters are kept constant in the simulations. Figure 8 shows the relationship between some input beam parameters and the transmission efficiency.

A large emittance which is indicative of a large beam size and divergence, will decrease the transmission efficiency. The transmission efficiency is approximately 95% with 6% energy spread when the emittance is 0.35 π mm mrad. This energy spread is much greater than that produced by the LEBT. When the beam current is 0.8 pmA, the transmission efficiency is maintained at 96%. This current tolerance satisfies the requirement of the accelerator and provides a large space for subsequent upgrading.

Except for the impact of a non-ideal input beam on the RFQ, there are some errors which result from fabrication,

Fig. 4 The final result of the fast-bunching design parameters as a function of position *z* (Color online)

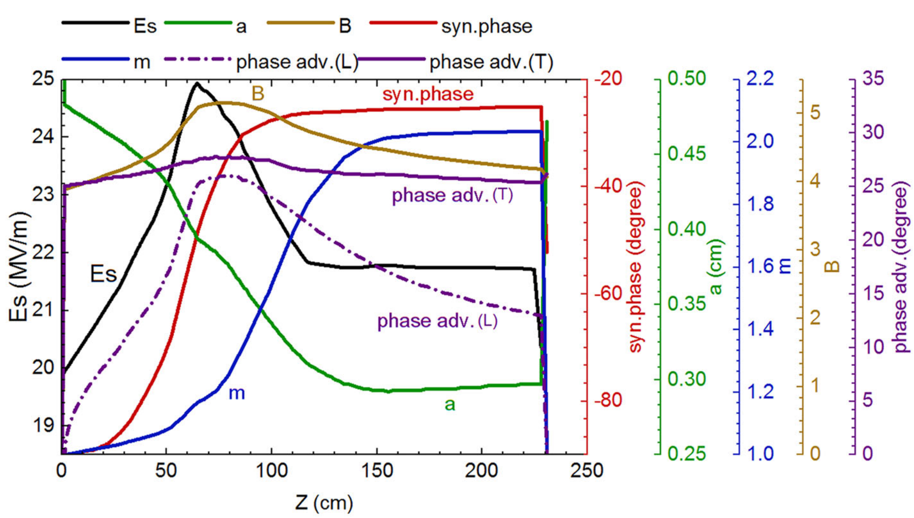

Table 3 Comparison of parameters between traditional design and fast-bunching design

Parameter	Traditional design	Fast-buncher design
Frequency (MHz)	162.5	162.5
Beam current (euA)	200	200
Input energy (keV/u)	8	8
Output energy (keV/u)	601.93	601.45
Duty factor (%)	1	1
Kilpatrick factor	1.82	1.83
Minimum aperture (a) (cm)	0.28	0.3
Average aperture ($r0$) (cm)	0.42	0.45
Input trans. emit. (π mm mrad)	0.200	0.200
Output trans. emit. (π mm mrad)	0.200	0.199
Output longitudinal emit. (π MeV deg)	0.434	0.242
Length of the vane (cm)	272.89	230.14
Transmission efficiency (%)	95.5	99.3

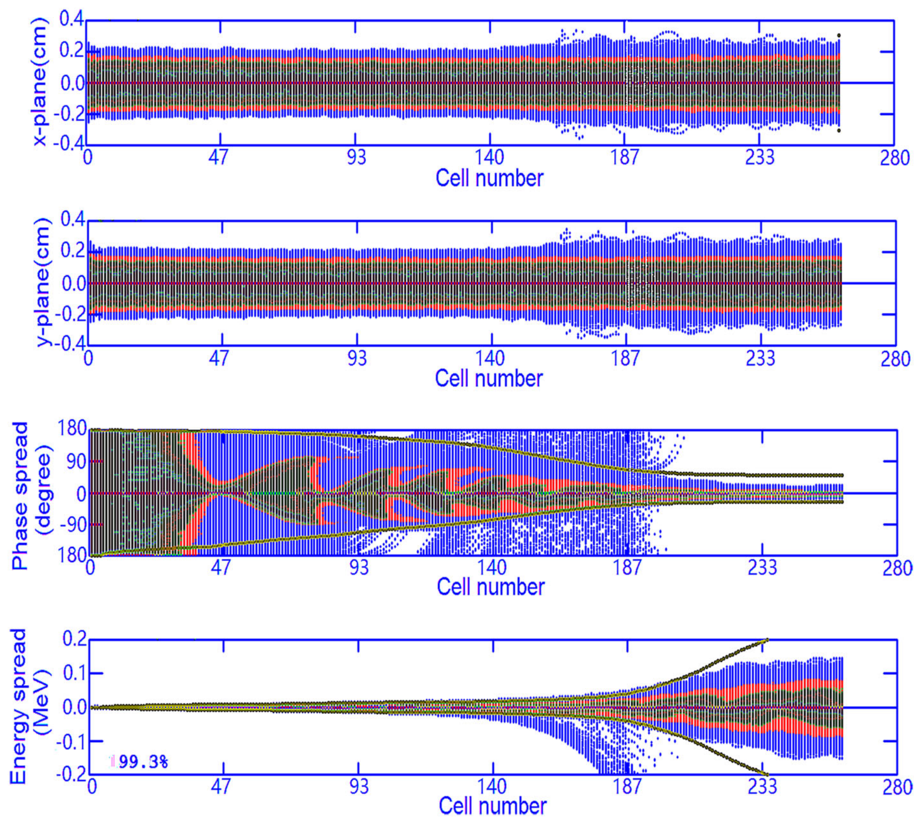

Fig. 5 Beam envelope evolution along the RFQ under final optimized design simulated by PARMTEQM. Plots from top to bottom are the beam profile in x- and y-planes, phase and energy spectra, respectively (Color online)

assembling, and operation. Some of these errors may adversely affect the beam transmission in the RFQ. As such, it is necessary to perform an error analysis of the RFQ. In this regard, we performed 1000 simulations using the TraceWin code. The error setting includes five items as shown in Table 4. The errors are uniformly distributed in the ranges listed in Table 4.

The dR value refers to the error of the electrode pole radius, and the d refers to the error of the depth of the modulation curve. Both of these values are set to 0.1 mm based on prior experience with SSC-Linac fabrication. The ϕ refers to the error of the RF phase, which is determined by the precision of the RF phase control system. The ΔT and ΔL are the cavity position offsets produced during installing, which are set by the precision of the collimation.

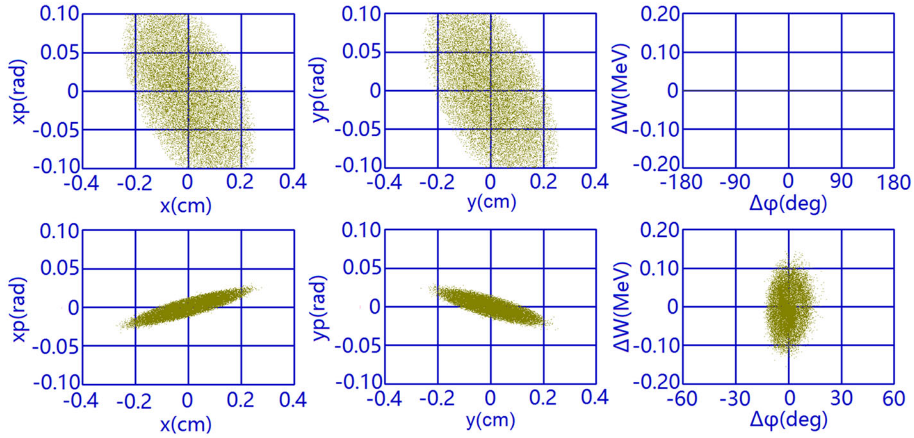

Fig. 6 Transverse phase space projection at the entrance and exit of the RFQ. The upper three figures refer to the entrance, while the lower three refer to the exit. For the input beam, zero energy spread and 360° phase width are assumed. The points in the top right box are located on the line ΔW = 0.00 (Color online)

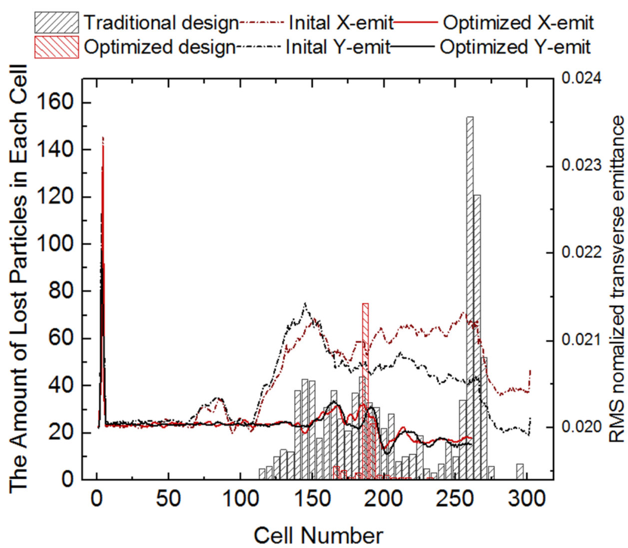

Fig. 7 Comparison of beam loss (shaded bar graphs) and transverse emittance growth (dashed and solid curves) between the traditional and optimized design (Color online)

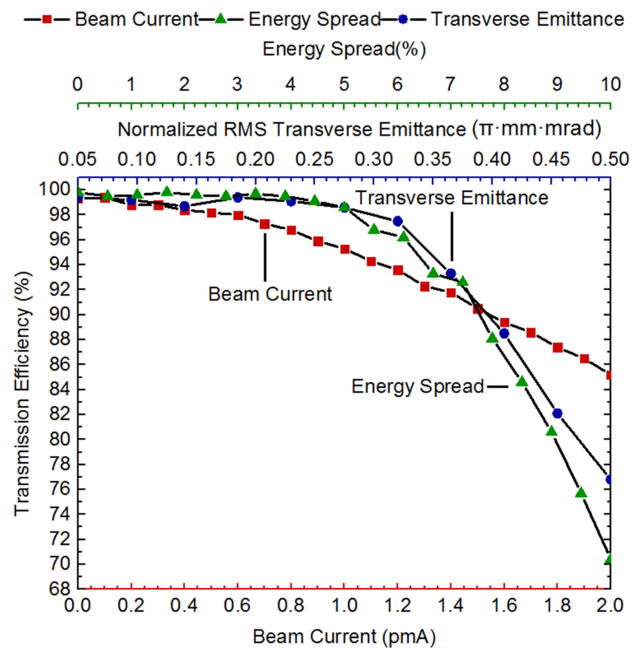

Fig. 8 Transmission efficiency of the RFQ versus input beam parameters. The red-square line represents the emittance. The green-triangle line represents the beam energy spread, and the blue-circle line represents the beam current (Color online)

Based on the analysis of 1000 sets of errors, the probability distribution of the beam loss is determined using TraceWin simulations as shown in Fig. 9. The calculated transmission efficiency is slightly higher than that of PARMTEQM, because the electric field and the beam loss criteria are different [23]. As shown in Fig. 9a, it is 70% more likely to maintain the transmission efficiency above 97% when the fabrication and operation errors are considered. In Fig. 9b, an emittance growth of less than 15% is highly feasible. This value will exceed not 30% when the RFQ error is taken into account. The emittance growth satisfies the operational requirement, and therefore, this dynamics design could be used for fabrication.

Table 4 The setting of the RFQ error analysis

Parameters	Range
Distribution	Uniformly
dR (mm)	± 0.1
d (mm)	± 0.1
ϕ (°)	± 1
ΔT (mm)	± 0.2
ΔL (mm)	± 0.2

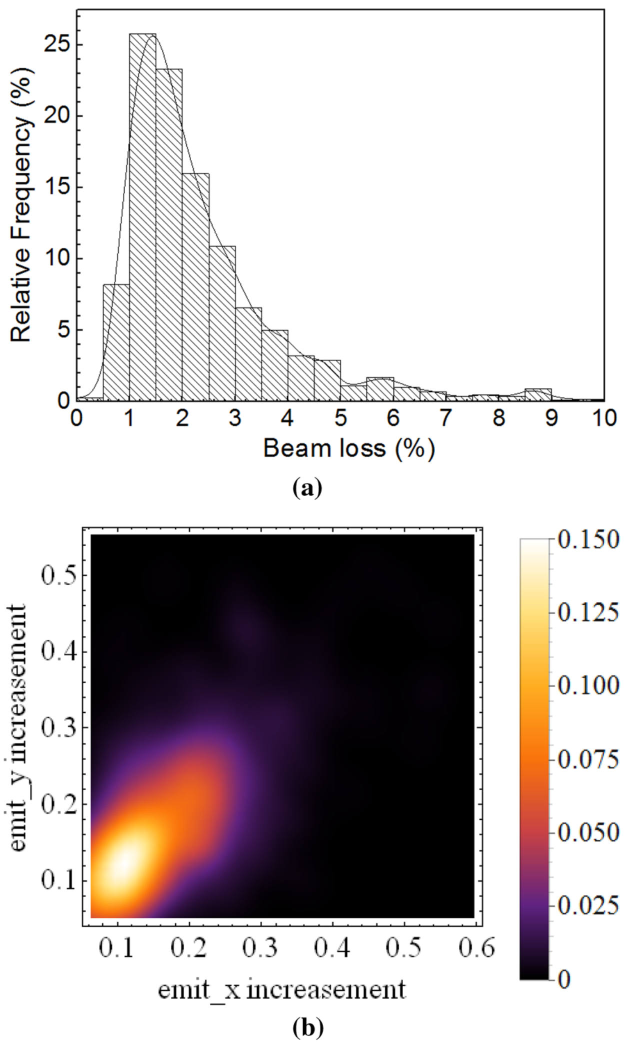

Fig. 9 The relative frequency of the beam loss and transverse emittance increase for the error setting (Color online)

4 Summary

A new RFQ design method which uses a fast-bunching section instead of the traditional GB section is developed for a compact, low-intensity linac. The design is constrained by the condition that the S parameter could be kept almost constant when the space-charge effect is not strong. In the case of IMP cancer therapy RFQ, very low beam loss is achieved using a fast longitudinal bunching process. Finally, bunching design is adopted to meet the strict requirements of a short length. This proposed method could benefit the next generation of RFQs for medical and nuclear physics applications where the current is relatively low, and the space-charge is not important.

Acknowledgements The authors would like to give special thanks to Prof. Yuan-Rong Lu at Peking University for his helpful suggestions, and to several other individuals of the Institute of Modern Physics, CAS, for their help and support.

References

1. T. Wangler, *RF Linear Accelerators* (Wiley, New York, 2008), p. 46
2. H. Eickhoff, R. Bar, A. Dolinskii, et al., HICAT—the German hospital-based light ion cancer therapy project. Paper presented at Particle Accelerator Conference, 2003. PAC 2003
3. K. Kawachi, T. Kanai, M. Endo et al., Radiation oncological facilities of the HIMAC. J. Jpn. Soc. Ther. Radiol. Oncol. **1**, 19–29 (1989)
4. T. Ohno, T. Kanai, S. Yamada et al., Carbon ion radiotherapy at the Gunma University Heavy Ion Medical Center: new facility set-up. Cancers **3**(4), 4046–4060 (2011). https://doi.org/10.3390/cancers3044046
5. T. Ohno, Particle radiotherapy with carbon ion beams. EPMA J. **4**(1), 9–9 (2013). https://doi.org/10.1186/1878-5085-4-9
6. J.C. Yang, J. Shi, W.P. Chai et al., Design of a compact structure cancer therapy synchrotron. Nucl. Inst. Methods Phys. Res. A **756**(16), 19–22 (2014). https://doi.org/10.1016/j.nima.2014.04.050
7. A. Kitagawa, T. Fujita, M. Muramatsu et al., Review on heavy ion radiotherapy facilities and related ion sources. Rev. Sci. Instrum. **81**(2), 295 (2010). https://doi.org/10.1063/1.3268510
8. G. Liu, Y.R. Lu, Y. He et al., Design of a CW high charge state heavy ion RFQ for SSC-LINAC. Nucl. Instrum. Methods Phys. Res. A **701**(3), 186–193 (2013). https://doi.org/10.1016/j.nima.2012.11.017
9. C. Li, L. Sun, Y. He et al., Conceptual design of LEBT and RFQ for the HIAF linac. Nucl. Instrum. Methods Phys. Res. A **729**, 426–433 (2013). https://doi.org/10.1016/j.nima.2013.06.019
10. C. Zhang, Z.Y. Guo, A. Schempp et al., Low-beam-loss design of a compact, high-current deuteron radio frequency quadrupole accelerator. Phys. Rev. Spec. Top. Accel. Beams **7**(10), 100101 (2004). https://doi.org/10.1103/PhysRevSTAB.7.100101
11. R. Gaur, P. Shrivastava, Beam dynamics and electromagnetic design studies of 3 MeV RFQ for SNS Programme. J. Electromag. Anal. Appl. **02**(09), 519–528 (2010). https://doi.org/10.4236/jemaa.2010.29068
12. C. Xiao, Y. He, Y.J. Yuan, et al. Particle-in-cell mode beam dynamics simulation of the low energy beam transport for the SSC-linac injector. Chinese Phys. C **35**(5), 500–504 (2011). https://doi.org/10.1088/1674-1137/35/5/019
13. K.R. Crandall, T.P. Wangler, L.M. Young, et al., RFQ design codes, LA-UR-96-1836
14. Y.S. Cho, Design of a 200-MHz RFQ for 3-MeV He beam irradiation. J. Korean Phys. Soc. **63**(7), 1327–1331 (2013). https://doi.org/10.3938/jkps.63.1327
15. X. Yan, K. Zhu, Y. Lu et al., Design of RFQ accelerator facility of PKUNIFTY. Phys. Proc. **26**, 79–87 (2012). https://doi.org/10.1016/j.nima.2010.12.028
16. R.A. Jameson, New linac technology for SSC, and beyond? Paper presented at International Conference on High-Energy Accelerators, Fermi National Accelerator Laboratory, Batavia, IL, Aug 2011
17. X.H. Zhang, Y.J. Yuan, J.W. Xia et al., Conceptional design of a heavy ion linac injector for HIRFL-CSRm. Chinese Phys. C **38**(6), 74–81 (2014). https://doi.org/10.1088/1674-1137/38/10/107002
18. M. Weiss, Turner S, in CERN Accelerator School : 5th Advanced Accelerator Physics Course, Rhodes, Greece, 20 Sep.-1 Oct. 1995, p. 974

19. S. Yamada, Buncher section optimization of heavy ion RFQ linacs, in *LASL Proceedings of the 1981 Linear Accelerator Conference* (1981), pp. 316–318
20. X.H. Zhang, Y.J. Yuan, J.W. Xia et al., Instability research of 53.667 MHz heavy ion RFQ. J. At. Energy Sci. Technol. **49**(5), 951–954 (2018). https://doi.org/10.7538/yzk.2015.49.05.0951
21. T. Sen, M.J. Syphers, Effect of power supply ripple on emittance growth in the collider, in *Proceedings of the Particle Accelerator Conference*, vol. 1 (IEEE, 1993), pp. 146–148
22. Y. Cao, J. Li, L.T. Sun et al., An all permanent magnet electron cyclotron resonance ion source for heavy ion therapy. Rev. Sci. Instrum. **85**(2), 02A960 (2014). https://doi.org/10.1063/1.4852335
23. K. Zhu, Y.R. Lu, X.J. Yin et al., The beam commissioning of a CW high charge state heavy ion RFQ. J. Nucl. Instrum. Methods Phys. Res. **794**(3), 113–121 (2015). https://doi.org/10.1016/j.nima.2015.05.012